

Tensor Ring Decomposition

Qibin Zhao, Guoxu Zhou, Shengli Xie, Liqing Zhang, Andrzej Cichocki *Fellow, IEEE*

Abstract—Tensor networks have in recent years emerged as the powerful tools for solving the large-scale optimization problems. One of the most popular tensor network is tensor train (TT) decomposition that acts as the building blocks for the complicated tensor networks. However, the TT decomposition highly depends on permutations of tensor dimensions, due to its strictly sequential multilinear products over latent cores, which leads to difficulties in finding the optimal TT representation. In this paper, we introduce a fundamental tensor decomposition model to represent a large dimensional tensor by a circular multilinear products over a sequence of low dimensional cores, which can be graphically interpreted as a cyclic interconnection of 3rd-order tensors, and thus termed as tensor ring (TR) decomposition. The key advantage of TR model is the circular dimensional permutation invariance which is gained by employing the trace operation and treating the latent cores equivalently. TR model can be viewed as a linear combination of TT decompositions, thus obtaining the powerful and generalized representation abilities. For optimization of latent cores, we present four different algorithms based on the sequential SVDs, ALS scheme, and block-wise ALS techniques. Furthermore, the mathematical properties of TR model are investigated, which shows that the basic multilinear algebra can be performed efficiently by using TR representations and the classical tensor decompositions can be conveniently transformed into the TR representation. Finally, the experiments on both synthetic signals and real-world datasets were conducted to evaluate the performance of different algorithms.

Index Terms—Tensor ring decomposition, tensor train decomposition, tensor networks, CP decomposition, Tucker decomposition, tensor rank



1 INTRODUCTION

TENSOR decompositions aim to represent a higher-order (or high-dimensional) tensor data by multilinear operations over the latent factors, which have attracted considerable attentions in a variety of fields including machine learning, signal processing, psychometric, chemometrics, quantum physics and brain science [1], [2]. Specifically, the Canonical Polyadic decomposition (CPD) [3], [4], [5], [6] can approximate an observed tensor by a sum of rank-one tensors, which requires $\mathcal{O}(dnr)$ parameters. The Tucker decomposition [7], [8], [9] attempts to approximate tensors by a core tensor and several factor matrices, which requires $\mathcal{O}(dnr + r^d)$ parameters. These two models have been widely investigated and applied in various real-world applications, e.g., [10], [11], [12], [13], [14], [15], [16], [17], [18], [19], [20], [21], [22]. In general, CPD provides a compact representation but with difficulties in finding the optimal solution, while Tucker is stable and flexible but its number of parameters scales exponentially to the tensor order.

Recently, tensor networks, considered as the generalization of tensor decompositions, have emerged as the potentially powerful tools for analysis of large-scale tensor data [23], [24], [25], [26]. The main concept is to transform a large-scale optimization problem into a set of small-scale

tractable optimization problems, which can be achieved by representing a higher-order tensor as the interconnected lower-order tensors [27], [28], [29]. The most popular tensor network is *tensor train / matrix product states* (TT/MPS) representation, which requires $\mathcal{O}(dnr^2)$ parameters and thus potentially allows for the efficient treatment of a higher dimensional tensor [30], [31], [32]. Another important tensor network is the hierarchical Tucker (HT) format [33], [34], in which a recursive, hierarchical construction of Tucker type is employed for low-dimensional representation. The usefulness of these tensor formats is currently being investigated for a variety of high-dimensional problems [35], [36]. For example, TT-format has been successfully applied to different kinds of large-scale problems in numerical analysis, which includes the optimization of Rayleigh quotient, e.g., *density matrix renormalization group* (DMRG) [37], [38], the eigenvalue or singular value problem [39], [40], and the approximate solution of linear systems, e.g., *alternating minimal energy* (AMEn) [41]. One main advantage of HT and TT formats lies in the fact that the representation of higher-order tensors is reduced to d tensors of order at most 3. Hence, the HT/TT formats are thus formally free from the curses of dimensionality. At the same time, new tensor formats have been proposed, e.g. the *quantized tensor train* (QTT) [42], [43] and the QTT-Tucker [44], which have been also applied to large-scale optimization problems [41], [45], [46].

Since TT decomposition acts as the building blocks for the complicated tensor networks, it is essentially important and necessary to investigate its properties deeply. The principle of TT decomposition is to approximate each tensor element by a sequential products of matrices, where the first and the last matrices are vectors to ensure the scalar output [31]. It was shown in [30] that TT decomposition with minimal possible compression ranks always exists and

- Q. Zhao is with Laboratory for Advanced Brain Signal Processing, RIKEN Brain Science Institute, Japan.
- G. Zhou is with the School of Automation at Guangdong University of Technology, Guangzhou 510006.
- S. Xie is with the School of Automation at Guangdong University of Technology, Guangzhou 510006.
- L. Zhang is with MOE-Microsoft Laboratory for Intelligent Computing and Intelligent Systems and Department of Computer Science and Engineering, Shanghai Jiao Tong University, China.
- A. Cichocki is with Laboratory for Advanced Brain Signal Processing, RIKEN Brain Science Institute, Japan and Systems Research Institute in Polish Academy of Science, Warsaw, Poland.

can be computed by a sequence of SVD decompositions, or by the cross approximation algorithm. In [32], [47], TT decomposition is optimized by a suitable generalization of the alternating least squares (ALS) algorithm and modified ALS (MALS) algorithm which facilitates the self-adaptation of ranks either by using SVDs or by employing a greedy algorithm. The tensor completion by optimizing the low-rank TT representations can be achieved by alternating directions fitting [48] or by nonlinear conjugate gradient scheme within the framework of Riemannian optimization [49]. Although TT format has been widely applied in numerical analysis and mathematic field, there are only few studies addressing its applications to real dataset in machine learning field, such as image classification and completion [50], [51], [52]. The limitations of TT decomposition include that i) the constraint on TT-ranks, i.e., $r_1 = r_{d+1} = 1$, leads to the limited representation ability and flexibility; ii) TT-ranks always have a fixed pattern, i.e., smaller for the border cores and larger for the middle cores, which might not be the optimum for specific data tensor; iii) the multilinear products of cores in TT must follow a strict order such that the optimized TT cores highly depend on the permutation of tensor dimensions. Hence, finding the optimal permutation remains a challenging problem.

By taking into account these limitations of TT decomposition, we introduce a new type of tensor decomposition which can be considered as a generalization of the TT model. First of all, we consider to relax the condition over TT-ranks, i.e., $r_1 = r_{d+1} = 1$, leading to the enhanced representation ability. Secondly, the strict ordering of multilinear products between cores should be alleviated. Third, the cores should be treated equivalently by making the model symmetric. To this end, we found these goals can be achieved by simply employing the trace operation. More specifically, we consider that each tensor element is approximated by performing a trace operation over the sequential multilinear products of cores. Since the trace operation ensures a scalar output, $r_1 = r_{d+1} = 1$ is not necessary. In addition, the cores can be circularly shifted and treated equivalently due to the properties of trace operation. By using the graphical illustration (see Fig. 1), this concept implies that the cores are interconnected circularly, which looks like a ring structure. Hence, we call this model as tensor ring (TR) decomposition and its cores as tensor ring (TR) representations. Although the similar concept has been mentioned and called MPS or tensor chain in few literatures [29], [42], [53], the algorithms and properties have not well explored yet. In this paper, the optimization algorithms for TR decomposition will be investigated, whose objective is to represent a higher-order tensor by the TR format that is potentially powerful for large-scale multilinear optimization problems.

The paper is organized as follows. In Section 2, the TR model is presented in several different forms together with its basic feature. Section 3 presents four different algorithms for TR decomposition. In Section 4, we demonstrate how the basic multilinear algebra can be performed by using the TR format. The relations with existing tensor decompositions are presented in Section 5. Section 6 shows experimental results on both synthetic and real-world dataset, followed by conclusion in Section 7.

2 TENSOR RING MODEL

The tensor ring (TR) decomposition aims to represent a high-order (or high-dimensional) tensor by a sequence of 3rd-order tensors that are multiplied circularly. Specifically, let \mathcal{T} be a d th-order tensor of size $n_1 \times n_2 \times \dots \times n_d$, denoted by $\mathcal{T} \in \mathbb{R}^{n_1 \times \dots \times n_d}$, TR representation is to decompose it into a sequence of latent tensors $\mathcal{Z}_k \in \mathbb{R}^{r_k \times n_k \times r_{k+1}}$, $k = 1, 2, \dots, d$, which can be expressed in an element-wise form given by

$$\begin{aligned} T(i_1, i_2, \dots, i_d) &= \text{Tr} \{ \mathbf{Z}_1(i_1) \mathbf{Z}_2(i_2) \dots \mathbf{Z}_d(i_d) \}, \\ &= \text{Tr} \left\{ \prod_{k=1}^d \mathbf{Z}_k(i_k) \right\}. \end{aligned} \quad (1)$$

$T(i_1, i_2, \dots, i_d)$ denotes (i_1, i_2, \dots, i_d) th element of the tensor. $\mathbf{Z}_k(i_k)$ denotes the i_k th lateral slice matrix of the latent tensor \mathcal{Z}_k , which is of size $r_k \times r_{k+1}$. Note that any two adjacent latent tensors, \mathcal{Z}_k and \mathcal{Z}_{k+1} , have an equivalent dimension r_{k+1} on their corresponding mode. The last latent tensor \mathcal{Z}_d is of size $r_d \times n_d \times r_1$, i.e., $r_{d+1} = r_1$, which ensures the product of these matrices is a square matrix. These prerequisites play key roles in TR decomposition, resulting in some important numeric properties. For simplicity, the latent tensor \mathcal{Z}_k can be also called k th-core (or node). The size of cores, $r_k, k = 1, 2, \dots, d$, collected and denoted by a vector $\mathbf{r} = [r_1, r_2, \dots, r_d]^T$ are called TR-ranks. From (1), we can observe that the $T(i_1, i_2, \dots, i_d)$ is equivalent to the trace of a sequential product of matrices $\{\mathbf{Z}_k(i_k)\}$. To further describe the concept, we can also rewrite (1) in the index form, which is

$$T(i_1, i_2, \dots, i_d) = \sum_{\alpha_1, \dots, \alpha_d=1}^{r_1, \dots, r_d} \prod_{k=1}^d \mathbf{Z}_k(\alpha_k, i_k, \alpha_{k+1}). \quad (2)$$

Note that $\alpha_{d+1} = \alpha_1$ due to the trace operation. $\forall k \in \{1, \dots, d\}, 1 \leq \alpha_k \leq r_k, 1 \leq i_k \leq n_k$, where k is the index of tensor modes (dimensions); α_k is the index of latent dimensions; and i_k is the index of data dimensions. From (2), we can also easily express TR decomposition in the tensor form, given by

$$\mathcal{T} = \sum_{\alpha_1, \dots, \alpha_d=1}^{r_1, \dots, r_d} \mathbf{z}_1(\alpha_1, \alpha_2) \circ \mathbf{z}_2(\alpha_2, \alpha_3) \circ \dots \circ \mathbf{z}_d(\alpha_d, \alpha_1), \quad (3)$$

where the symbol ' \circ ' denotes the outer product of vectors and $\mathbf{z}_k(\alpha_k, \alpha_{k+1}) \in \mathbb{R}^{n_k}$ denotes the (α_k, α_{k+1}) th mode-2 fiber of tensor \mathcal{Z}_k . This indicates that the whole tensor can be decomposed into a sum of rank-1 tensors that are generated by d vectors taken from each core respectively. The number of parameters in TR representation is $\mathcal{O}(dnr^2)$, which is linear to the tensor order d .

The TR representation can be also illustrated graphically by a linear tensor network as shown in Fig. 1. The node represents a tensor (including matrix and vector) whose order is denoted by the number of edges. The number beside the edges specifies the size of each mode (or dimension). The connection between two nodes denotes a multilinear product operator between two tensors on a specific mode, also called tensor contraction, which corresponds to the summation over the indices of that mode. As we can see

The subchain tensor by merging all cores except k th core \mathcal{Z}_k , i.e., $\mathcal{Z}_{k+1}, \dots, \mathcal{Z}_d, \mathcal{Z}_1, \dots, \mathcal{Z}_{k-1}$, is denoted by $\mathcal{Z}^{\neq k} \in \mathbb{R}^{r_{k+1} \times \prod_{j=1, j \neq k}^d n_j \times r_k}$ whose slice matrices are defined by

$$\mathbf{Z}^{\neq k}(\overline{i_{k+1} \dots i_d i_1 \dots i_{k-1}}) = \prod_{j=k+1}^d \mathbf{Z}_j(i_j) \prod_{j=1}^{k-1} \mathbf{Z}_j(i_j). \quad (12)$$

Analogously, we can also define subchains of $\mathcal{Z}^{\leq k}$, $\mathcal{Z}^{\geq k}$ and $\mathcal{Z}^{\neq(k, k+1)}$ in the same way. Note that a special subchain by merging all cores is denoted by $\mathcal{Z}^{(1:d)}$ of size $r_1 \times \prod_{j=1}^d n_j \times r_1$ whose mode-2 fibers $\mathbf{Z}^{(1:d)}(\alpha_1, :, \alpha_1)$, $\alpha_1 = 1, \dots, r_1$ can be represented as TT representations, respectively.

3.1 Sequential SVDs algorithm

We propose the first algorithm for computing the TR decomposition using d sequential SVDs. This algorithm will be called TR-SVD algorithm.

Theorem 3.4. *Let us assume \mathcal{T} can be represented by a TR decomposition. If the k -unfolding matrix $\mathbf{T}_{\langle k \rangle}$ has $\text{Rank}(\mathbf{T}_{\langle k \rangle}) = R_{k+1}$, then there exists a TR decomposition with TR-ranks \mathbf{r} which satisfies that $\exists k, r_1 r_{k+1} \leq R_{k+1}$.*

Proof. We can express TR decomposition in the form of k -unfolding matrix,

$$\begin{aligned} \mathbf{T}_{\langle k \rangle}(\overline{i_1 \dots i_k, i_{k+1} \dots i_d}) &= \text{Tr} \{ \mathbf{Z}_1(i_1) \mathbf{Z}_2(i_2) \dots \mathbf{Z}_d(i_d) \} \\ &= \text{Tr} \left\{ \prod_{j=1}^k \mathbf{Z}_j(i_j) \prod_{j=k+1}^d \mathbf{Z}_j(i_j) \right\} \\ &= \left\langle \text{vec} \left(\prod_{j=1}^k \mathbf{Z}_j(i_j) \right), \text{vec} \left(\prod_{j=d}^{k+1} \mathbf{Z}_j^T(i_j) \right) \right\rangle. \end{aligned} \quad (13)$$

According to the definitions in (10)(11), (13) can be also rewritten as

$$\begin{aligned} \mathbf{T}_{\langle k \rangle}(\overline{i_1 \dots i_k, i_{k+1} \dots i_d}) \\ = \sum_{\alpha_1 \alpha_{k+1}} \mathbf{Z}^{\leq k}(\overline{i_1 \dots i_k, \alpha_1 \alpha_{k+1}}) \mathbf{Z}^{\geq k}(\overline{\alpha_1 \alpha_{k+1}, i_{k+1} \dots i_d}). \end{aligned} \quad (14)$$

Hence, we can obtain that $\mathbf{T}_{\langle k \rangle} = \mathbf{Z}_{(2)}^{\leq k} (\mathbf{Z}_{(2)}^{\geq k})^T$, where the subchain $\mathbf{Z}_{(2)}^{\leq k}$ is of size $\prod_{j=1}^k n_j \times r_1 r_{k+1}$, and $\mathbf{Z}_{(2)}^{\geq k}$ is of size $\prod_{j=k+1}^d n_j \times r_1 r_{k+1}$. Since the rank of $\mathbf{T}_{\langle k \rangle}$ is R_{k+1} , we can obtain that $r_1 r_{k+1} \leq R_{k+1}$. \square

For TT-SVD algorithm, we usually need to choose a specific mode as the start point (e.g., the first mode). According to (13)(14), TR decomposition can be easily written as

$$\mathbf{T}_{\langle 1 \rangle}(\overline{i_1, i_2 \dots i_d}) = \sum_{\alpha_1, \alpha_2} \mathbf{Z}^{\leq 1}(\overline{i_1, \alpha_1 \alpha_2}) \mathbf{Z}^{\geq 1}(\overline{\alpha_1 \alpha_2, i_2 \dots i_d}). \quad (15)$$

Since the low-rank approximation of $\mathbf{T}_{\langle 1 \rangle}$ can be easily obtained by the truncated SVD, which is

$$\mathbf{T}_{\langle 1 \rangle} = \mathbf{U} \Sigma \mathbf{V}^T + \mathbf{E}_1, \quad (16)$$

the first core \mathcal{Z}_1 (i.e., $\mathcal{Z}^{\leq 1}$) of size $r_1 \times n_1 \times r_2$ can be obtained by the proper reshaping and permutation of \mathbf{U}

and the subchain $\mathcal{Z}^{\geq 1}$ of size $r_2 \times \prod_{j=2}^d n_j \times r_1$ is obtained by the proper reshaping and permutation of $\Sigma \mathbf{V}^T$, which corresponds to the rest $d-1$ dimensions of \mathcal{T} . Subsequently, we can further reshape the subchain $\mathcal{Z}^{\geq 1}$ as a matrix $\mathbf{Z}^{\geq 1} \in \mathbb{R}^{r_2 n_2 \times \prod_{j=3}^d n_j r_1}$ which thus can be written as

$$\mathbf{Z}^{\geq 1}(\overline{\alpha_2 i_2, i_3 \dots i_d \alpha_1}) = \sum_{\alpha_3} \mathbf{Z}_2(\overline{\alpha_2 i_2, \alpha_3}) \mathbf{Z}^{\geq 2}(\overline{\alpha_3, i_3 \dots i_d \alpha_1}). \quad (17)$$

By applying truncated SVD, i.e., $\mathbf{Z}^{\geq 1} = \mathbf{U} \Sigma \mathbf{V}^T + \mathbf{E}_2$, we can obtain the second core \mathcal{Z}_2 of size $(r_2 \times n_2 \times r_3)$ by appropriately reshaping \mathbf{U} and the subchain $\mathcal{Z}^{\geq 2}$ by proper reshaping of $\Sigma \mathbf{V}^T$. This procedure can be performed sequentially to obtain all d cores $\mathcal{Z}_k, k = 1, \dots, d$.

As proved in [31], the approximation error by using such sequential SVDs is given by

$$\|\mathcal{T} - \mathfrak{R}(\mathcal{Z}_1, \mathcal{Z}_2, \dots, \mathcal{Z}_d)\|_F \leq \sqrt{\sum_{k=1}^{d-1} \|\mathbf{E}_k\|_F^2}. \quad (18)$$

Hence, given a prescribed relative error ϵ_p , the truncation threshold δ can be set to $\frac{\epsilon_p}{\sqrt{d-1}} \|\mathcal{T}\|_F$. However, considering that $\|\mathbf{E}_1\|_F$ corresponds to two ranks including both r_1 and r_2 , while $\|\mathbf{E}_k\|_F, \forall k > 1$ correspond to only one rank r_{k+1} . Therefore, we modify the truncation threshold as

$$\delta_k = \begin{cases} \sqrt{2} \epsilon_p \|\mathcal{T}\|_F / \sqrt{d}, & k = 1, \\ \epsilon_p \|\mathcal{T}\|_F / \sqrt{d}, & k > 1. \end{cases} \quad (19)$$

Finally, the TR-SVD algorithm is summarized in Alg. 1.

Algorithm 1 TR-SVD

Input: A d th-order tensor \mathcal{T} of size $(n_1 \times \dots \times n_d)$ and the prescribed relative error ϵ_p .

Output: Cores $\mathcal{Z}_k, k = 1, \dots, d$ of TR decomposition and the TR-ranks \mathbf{r} .

- 1: Compute truncation threshold δ_k for $k = 1$ and $k > 1$.
- 2: Choose one mode as the start point (e.g., the first mode) and obtain the 1-unfolding matrix $\mathbf{T}_{\langle 1 \rangle}$.
- 3: Low-rank approximation by applying δ_1 -truncated SVD: $\mathbf{T}_{\langle 1 \rangle} = \mathbf{U} \Sigma \mathbf{V}^T + \mathbf{E}_1$.
- 4: Split ranks r_1, r_2 by

$$\min_{r_1, r_2} \|r_1 - r_2\|, \quad \text{s.t.} \quad r_1 r_2 = \text{rank}_{\delta_1}(\mathbf{T}_{\langle 1 \rangle}).$$

- 5: $\mathcal{Z}_1 \leftarrow \text{permute}(\text{reshape}(\mathbf{U}, [n_1, r_1, r_2]), [2, 1, 3])$.
- 6: $\mathcal{Z}^{\geq 1} \leftarrow \text{permute}(\text{reshape}(\Sigma \mathbf{V}^T, [r_1, r_2, \prod_{j=2}^d n_j]), [2, 3, 1])$.
- 7: **for** $k = 2$ to $d-1$ **do**
- 8: $\mathbf{Z}^{\geq k-1} = \text{reshape}(\mathcal{Z}^{\geq k-1}, [r_k n_k, n_{k+1} \dots n_d r_1])$.
- 9: Compute δ_k -truncated SVD:

$$\mathbf{Z}^{\geq k-1} = \mathbf{U} \Sigma \mathbf{V}^T + \mathbf{E}_k.$$

- 10: $r_{k+1} \leftarrow \text{rank}_{\delta_k}(\mathbf{Z}^{\geq k-1})$.
 - 11: $\mathcal{Z}_k \leftarrow \text{reshape}(\mathbf{U}, [r_k, n_k, r_{k+1}])$.
 - 12: $\mathcal{Z}^{\geq k} \leftarrow \text{reshape}(\Sigma \mathbf{V}^T, [r_{k+1}, \prod_{j=k+1}^d n_j, r_1])$.
 - 13: **end for**
-

The cores obtained by TR-SVD algorithm are left-orthogonal, which is $\mathbf{Z}_{(k(2))}^T \mathbf{Z}_{(k(2))} = \mathbf{I}$, for $k = 2, \dots, d-1$. It should be noted that TR-SVD is a non-recursive algorithm that does not need iterations for convergence. However, it

might obtain different representations by choosing a different mode as the start point. This indicates that TR-ranks \mathbf{r} is not necessary to be the global optimum in TR-SVD. Therefore, we consider to develop other algorithms that can find the optimum TR-ranks and are independent with the start point.

3.2 ALS algorithm

In this section, we introduce an algorithm for TR decomposition by employing alternating least squares (ALS). The ALS algorithm has been widely applied to most tensor decomposition models such as CP and Tucker decompositions [1], [32]. The main concept of ALS is optimizing one core while the other cores are fixed, and this procedure will be repeated until some convergence criterion is satisfied. Given a d th-order tensor \mathcal{T} , our goal is to optimize the cores with a given TR-ranks \mathbf{r} , i.e.,

$$\min_{\mathcal{Z}_1, \dots, \mathcal{Z}_d} \|\mathcal{T} - \mathfrak{R}(\mathcal{Z}_1, \dots, \mathcal{Z}_d)\|_F. \quad (20)$$

Theorem 3.5. *Given a TR decomposition $\mathcal{T} = \mathfrak{R}(\mathcal{Z}_1, \dots, \mathcal{Z}_d)$, its mode- k unfolding matrix can be written as*

$$\mathbf{T}_{[k]} = \mathbf{Z}_{k(2)} \left(\mathbf{Z}_{[2]}^{\neq k} \right)^T, \quad (21)$$

where $\mathbf{Z}^{\neq k}$ is a subchain obtained by merging $d - 1$ cores, which is defined in (12).

Proof. According to the TR definition in (2), we have

$$\begin{aligned} & T(i_1, i_2, \dots, i_d) \\ &= \sum_{\alpha_1, \dots, \alpha_d} Z_1(\alpha_1, i_1, \alpha_2) Z_2(\alpha_2, i_2, \alpha_3) \cdots Z_d(\alpha_d, i_d, \alpha_1) \\ &= \sum_{\alpha_k, \alpha_{k+1}} \left\{ Z_k(\alpha_k, i_k, \alpha_{k+1}) \sum_{\substack{\alpha_1, \dots, \alpha_{k-1} \\ \alpha_{k+2}, \dots, \alpha_d}} Z_{k+1}(\alpha_{k+1}, i_{k+1}, \alpha_{k+2}) \right. \\ &\quad \left. \cdots Z_d(\alpha_d, i_d, \alpha_1) Z_1(\alpha_1, i_1, \alpha_2) \cdots Z_{k-1}(\alpha_{k-1}, i_{k-1}, \alpha_k) \right\} \\ &= \sum_{\alpha_k, \alpha_{k+1}} \left\{ Z_k(\alpha_k, i_k, \alpha_{k+1}) Z^{\neq k}(\alpha_{k+1}, \overline{i_{k+1} \cdots i_d i_1 \cdots i_{k-1}}, \alpha_k) \right\}. \end{aligned} \quad (22)$$

Hence, the mode- k unfolding matrix of \mathcal{T} can be expressed by

$$\begin{aligned} \mathbf{T}_{[k]}(i_k, \overline{i_{k+1} \cdots i_d i_1 \cdots i_{k-1}}) &= \sum_{\alpha_k \alpha_{k+1}} \left\{ Z_k(i_k, \overline{\alpha_k \alpha_{k+1}}) \right. \\ &\quad \left. Z^{\neq k}(\overline{\alpha_k \alpha_{k+1}}, \overline{i_{k+1} \cdots i_d i_1 \cdots i_{k-1}}) \right\}. \end{aligned} \quad (23)$$

This indicates a product of two matrices. By applying different mode- k unfolding operations, we can easily justify the formula in (21). \square

Based on Theorem 3.5, the objective function in (20) can be optimized by solving d subproblems alternatively. More specifically, having fixed all but one core, the problem reduces to a linear least squares problem, which is

$$\min_{\mathbf{Z}_{k(2)}} \left\| \mathbf{T}_{[k]} - \mathbf{Z}_{k(2)} \left(\mathbf{Z}_{[2]}^{\neq k} \right)^T \right\|_F, \quad k = 1, \dots, d. \quad (24)$$

Algorithm 2 TR-ALS

Input: A d th-order tensor \mathcal{T} of size $(n_1 \times \cdots \times n_d)$ and the predefined TR-ranks \mathbf{r} .

Output: Cores $\mathcal{Z}_k, k = 1, \dots, d$ of TR decomposition.

- 1: Initialize $\mathcal{Z}_k \in \mathbb{R}^{r_k \times n_k \times r_{k+1}}$ for $k = 1, \dots, d$ as random tensors from Gaussian distribution.
- 2: **repeat**
- 3: **for** $k = 1$ to d **do**
- 4: Compute the subchain $\mathbf{Z}^{\neq k}$ by using (12).
- 5: Obtain $\mathbf{Z}_{[2]}^{\neq k}$ of size $\prod_{j=1}^d n_j / n_k \times r_k r_{k+1}$.
- 6: $\mathbf{Z}_{k(2)} \leftarrow \arg \min \|\mathbf{T}_{[k]} - \mathbf{Z}_{k(2)} (\mathbf{Z}_{[2]}^{\neq k})^T\|_F$.
- 7: Normalize columns of $\mathbf{Z}_{k(2)}$, if $k \neq d$.
- 8: $\mathcal{Z}_k \leftarrow \text{permute}(\text{reshape}(\mathbf{Z}_{k(2)}, [n_k, r_k, r_{k+1}]), [2, 1, 3])$.
- 9: Relative error $\epsilon \leftarrow \|\mathcal{T} - \mathfrak{R}(\mathcal{Z}_1, \dots, \mathcal{Z}_d)\| / \|\mathcal{T}\|_F$
- 10: **end for**
- 11: **until** Relative changes of ϵ is smaller than a specific threshold (e.g. 10^{-6}), or maximum number of iterations is reached.

Therefore, TR composition can be performed by ALS optimizations, which is called TR-ALS algorithm. The detailed procedure is shown in Alg. 2.

The cores can be initialized randomly with specified TR-ranks. The iterations repeat until some combination of stopping conditions is satisfied. Possible stopping conditions include the following: little or no improvement in the objective function; the value of objective function being smaller than a specific threshold; a predefined maximum number of iterations is reached. The normalization is performed on all cores except the last one that absorbs the weights. It should be noted that the cores are not necessary to be orthogonal in TR-ALS.

3.3 ALS with adaptive ranks

One important limitation of TR-ALS algorithm is that TR-ranks must be specified and fixed, which may make the algorithm difficult to obtain a desired accuracy. Although we can try different TR-ranks and select the best one, the computation cost will dramatically increase due to the large number of possibilities when high dimensional tensors are considered. Therefore, we attempt to develop an ALS algorithm for TR decomposition with adaptive ranks, which is simply called ALSAR algorithm.

The ALSAR algorithm is initialized with equivalent TR-ranks, i.e., $r_1 = r_2 = \cdots = r_d = 1$. The core tensors $\mathcal{Z}_k, k = 1, \dots, d$ are initialized by random tensors which are of size $1 \times n_k \times 1$. For optimization of each core tensor \mathcal{Z}_k , it was firstly updated according to ALS scheme, yielding the updated approximation error ϵ_{old} . Then, we attempt to increase the rank by $r_{k+1} \leftarrow r_{k+1} + 1$, which implies that $\mathcal{Z}_k, \mathcal{Z}_{k+1}$ must be updated with the increased sizes. More specifically, based on the modified \mathcal{Z}_{k+1} by adding more random entries, \mathcal{Z}_k is updated again yielding the new approximation error ϵ_{new} . If the improvement of approximation error by increasing the rank r_{k+1} satisfies a specific criteria, then the increased rank is accepted otherwise it is rejected. The acceptance criteria can be simply expressed by

$$|\epsilon_{old} - \epsilon_{new}| > \tau |\epsilon_{old} - \epsilon_p|, \quad (25)$$

where ϵ_p denotes the desired approximation error, and τ denotes the threshold for accepting the increased rank. The reasonable choices for τ vary between $10^{-2}/d$ and $10^{-3}/d$. This procedure will be repeated until the desired approximation error is reached. The detailed algorithm is summarized in Alg. 3.

This algorithm is intuitive and heuristic. During the optimization procedure, the corresponding rank is tentatively increased followed by a decision making based on the acceptance criterion. Hence, it can achieve an arbitrary approximation error ϵ_p by rank adaptation. However, since the step of rank increasing is only one at each iteration, it might need many iterations to achieve the desired accuracy if TR-ranks are relatively large.

Algorithm 3 TR-ALSAR

Input: A d -dimensional tensor \mathcal{T} of size $(n_1 \times \dots \times n_d)$ and the prescribed relative error ϵ_p .

Output: Cores \mathcal{Z}_k and TR-ranks $r_k, k = 1, \dots, d$.

- 1: Initialize $r_k = 1$ for $k = 1, \dots, d$.
 - 2: Initialize $\mathcal{Z}_k \in \mathbb{R}^{r_k \times n_k \times r_{k+1}}$ for $k = 1, \dots, d$.
 - 3: **repeat**
 - 4: **for** $k = 1$ to d **do**
 - 5: $\mathbf{Z}_{k(2)} \leftarrow \arg \min \|\mathbf{T}_{[k]} - \mathbf{Z}_{k(2)}(\mathbf{Z}_{[2]}^{\neq k})^T\|_F$.
 - 6: Evaluate relative error ϵ_{old} .
 - 7: $r_{k+1} \leftarrow r_{k+1} + 1$.
 - 8: Increase the size of \mathcal{Z}_{k+1} by random samples.
 - 9: Repeat the steps 5-7 and evaluate the error ϵ_{new} .
 - 10: Determine $\mathbf{Z}_{k(2)}$ and r_{k+1} according to the specific acceptance criterion.
 - 11: Normalize columns of $\mathbf{Z}_{k(2)}$, if $k \neq d$.
 - 12: $\mathcal{Z}_k \leftarrow \text{permute}(\text{reshape}(\mathbf{Z}_{k(2)}, [n_k, r_k, r_{k+1}]), [2, 1, 3])$:
 - 13: **end for**
 - 14: **until** The desired approximation accuracy is achieved, i.e., $\epsilon \leq \epsilon_p$.
-

3.4 Block-wise ALS algorithm

In this section, we propose a computationally efficient block-wise ALS (BALS) algorithm by utilizing truncated SVD, which facilitates the self-adaptation of ranks. The main idea is to perform the blockwise optimization followed by the separation of block into individual cores. To achieve this, we consider to merge two linked cores, e.g., $\mathcal{Z}_k, \mathcal{Z}_{k+1}$, into a block (or subchain) $\mathcal{Z}^{(k,k+1)} \in \mathbb{R}^{r_k \times n_k \times n_{k+1} \times r_{k+2}}$ (see definition in (9)). Thus, the subchain $\mathcal{Z}^{(k,k+1)}$ can be optimized while leaving all cores except $\mathcal{Z}_k, \mathcal{Z}_{k+1}$ fixed. Subsequently, the subchain $\mathcal{Z}^{(k,k+1)}$ can be reshaped into $\tilde{\mathcal{Z}}^{(k,k+1)} \in \mathbb{R}^{r_k n_k \times n_{k+1} r_{k+2}}$ and separated into a left-orthonormal core \mathcal{Z}_k and \mathcal{Z}_{k+1} by a truncated SVD,

$$\tilde{\mathcal{Z}}^{(k,k+1)} = \mathbf{U}\Sigma\mathbf{V}^T = \mathbf{Z}_{k(2)}\mathbf{Z}_{k+1(1)}, \quad (26)$$

where $\mathbf{Z}_{k(2)} \in \mathbb{R}^{r_k n_k \times r_{k+1}}$ is the 2-unfolding matrix of core \mathcal{Z}_k , which can be set to \mathbf{U} , while $\mathbf{Z}_{k+1(1)} \in \mathbb{R}^{r_{k+1} \times n_{k+1} r_{k+2}}$ is the 1-unfolding matrix of core \mathcal{Z}_{k+1} , which can be set to $\Sigma\mathbf{V}^T$. This procedure thus move on to optimize the next block cores $\mathcal{Z}^{(k+1,k+2)}, \dots, \mathcal{Z}^{(d-1,d)}, \mathcal{Z}^{(d,1)}$ successively in the similar way. Note that since TR model is circular, the d th core can be also merged with the first core yielding the block core $\mathcal{Z}^{(d,1)}$.

The key advantage of BALS algorithm is the rank adaptation which can be achieved simply by separating the block core into two cores via truncated SVD, as shown in (26). The truncated rank r_{k+1} can be chosen such that the approximation error is below a certain threshold. One possible choice is to use the same threshold as in TR-SVD algorithm, i.e., δ_k described in (19). However, the empirical experience show that this threshold often leads to overfitting and the truncated rank is higher than the optimum rank. This is because that the updated block $\mathcal{Z}^{(k,k+1)}$ during ALS iterations is not a closed form solution and many iterations are necessary for convergence. To relieve this problem, we choose the truncation threshold based on both the current and the desired approximation errors, which is

$$\delta = \max \left\{ \epsilon \|\mathcal{T}\|_F / \sqrt{d}, \epsilon_p \|\mathcal{T}\|_F / \sqrt{d} \right\}. \quad (27)$$

The details of BALS algorithm are described in Alg. 4.

Algorithm 4 TR-BALS

Input: A d -dimensional tensor \mathcal{T} of size $(n_1 \times \dots \times n_d)$ and the prescribed relative error ϵ_p .

Output: Cores \mathcal{Z}_k and TR-ranks $r_k, k = 1, \dots, d$.

- 1: Initialize $r_k = 1$ for $k = 1, \dots, d$.
 - 2: Initialize $\mathcal{Z}_k \in \mathbb{R}^{r_k \times n_k \times r_{k+1}}$ for $k = 1, \dots, d$.
 - 3: **repeat** $k \in \text{circular}\{1, 2, \dots, d\}$;
 - 4: Compute the subchain $\mathcal{Z}^{\neq(k,k+1)}$ by using (12).
 - 5: Obtain the mode-2 unfolding matrix $\mathbf{Z}_{[2]}^{\neq(k,k+1)}$ of size $\prod_{j=1}^d n_j / (n_k n_{k+1}) \times r_k r_{k+2}$.
 - 6: $\mathbf{Z}_{(2)}^{(k,k+1)} \leftarrow \arg \min \left\| \mathbf{T}_{[k]} - \mathbf{Z}_{(2)}^{(k,k+1)} \left(\mathbf{Z}_{[2]}^{\neq(k,k+1)} \right)^T \right\|_F$.
 - 7: Tensorization of mode-2 unfolding matrix

$$\mathcal{Z}^{(k,k+1)} \leftarrow \text{folding}(\mathbf{Z}_{(2)}^{(k,k+1)}).$$
 - 8: Reshape the block core by

$$\tilde{\mathcal{Z}}^{(k,k+1)} \leftarrow \text{reshape}(\mathcal{Z}^{(k,k+1)}, [r_k n_k \times n_{k+1} r_{k+2}]).$$
 - 9: Low-rank approximation by δ -truncated SVD

$$\tilde{\mathcal{Z}}^{(k,k+1)} = \mathbf{U}\Sigma\mathbf{V}^T.$$
 - 10: $\mathcal{Z}_k \leftarrow \text{reshape}(\mathbf{U}, [r_k, n_k, r_{k+1}])$.
 - 11: $\mathcal{Z}_{k+1} \leftarrow \text{reshape}(\Sigma\mathbf{V}^T, [r_{k+1}, n_{k+1}, r_{k+2}])$.
 - 12: $r_{k+1} \leftarrow \text{rank}_\delta(\tilde{\mathcal{Z}}^{(k,k+1)})$.
 - 13: $k \leftarrow k + 1$.
 - 14: **until** The desired approximation accuracy is achieved, i.e., $\epsilon \leq \epsilon_p$.
-

3.5 Discussions on the proposed algorithms

We briefly summarize and discuss the proposed algorithms as follows. TR-SVD algorithm is generally efficient in computation due to its non-recursion property and it can approximate an arbitrary tensor as close as possible. However, its obtained TR-ranks $[r_1, \dots, r_d]$ always follow a specific pattern, i.e., smaller ranks on the both sides and larger ranks in the middle, which might not suitable to the observed data. The other three algorithms are based on ALS framework, resulting in that the optimum TR-ranks only depend on the observed data while the recursive procedure leads to the slow convergence. TR-ALS is stable but requires TR-ranks to be fixed and manually given. TR-ALSAL is able

to adapt TR-ranks during optimization, but requires many iterations. TR-BALS enables us to find the optimum TR-ranks efficiently without dramatically increasing the computational cost.

4 PROPERTIES OF TR REPRESENTATION

In this section, we discuss some interesting properties of TR representation. By assuming that tensor data have been already represented as TR decompositions, i.e., a sequence of third-order cores, we justify and demonstrate that the basic operations on tensors, such as *addition*, *multilinear product*, *Hadamard product*, *inner product* and *Frobenius norm*, can be performed efficiently by the appropriate operations on each individual cores. These properties are crucial and essentially important for processing large-scale or large-dimensional tensors, due to the ability of converting a large problem w.r.t. the original tensor into many small problems w.r.t. individual cores.

Theorem 4.1. *Let \mathcal{T}_1 and \mathcal{T}_2 be d th-order tensors of size $n_1 \times \dots \times n_d$. If the TR decompositions of these two tensors are $\mathcal{T}_1 = \mathfrak{R}(\mathcal{Z}_1, \dots, \mathcal{Z}_d)$ where $\mathcal{Z}_k \in \mathbb{R}^{r_k \times n_k \times r_{k+1}}$ and $\mathcal{T}_2 = \mathfrak{R}(\mathcal{Y}_1, \dots, \mathcal{Y}_d)$, where $\mathcal{Y}_k \in \mathbb{R}^{s_k \times n_k \times s_{k+1}}$, then the addition of these two tensors, $\mathcal{T}_3 = \mathcal{T}_1 + \mathcal{T}_2$, can be also represented in the TR format given by $\mathcal{T}_3 = \mathfrak{R}(\mathcal{X}_1, \dots, \mathcal{X}_d)$, where $\mathcal{X}_k \in \mathbb{R}^{q_k \times n_k \times q_{k+1}}$ and $q_k = r_k + s_k$. Each core \mathcal{X}_k can be computed by*

$$\mathbf{X}_k(i_k) = \begin{pmatrix} \mathbf{Z}_k(i_k) & 0 \\ 0 & \mathbf{Y}_k(i_k) \end{pmatrix}, \quad i_k = 1, \dots, n_k, \quad (28)$$

Proof. According to the definition of TR decomposition, and the cores shown in (28), the (i_1, \dots, i_d) th element of tensor \mathcal{T}_3 can be written as

$$\begin{aligned} T_3(i_1, \dots, i_d) &= \text{Tr}(\mathbf{X}_1(i_1) \dots \mathbf{X}_d(i_d)) \\ &= \text{Tr} \begin{pmatrix} \prod_{k=1}^d \mathbf{Z}_k(i_k) & 0 \\ 0 & \prod_{k=1}^d \mathbf{Y}_k(i_k) \end{pmatrix} \\ &= \text{Tr} \left(\prod_{k=1}^d \mathbf{Z}_k(i_k) \right) + \text{Tr} \left(\prod_{k=1}^d \mathbf{Y}_k(i_k) \right) \\ &= T_1(i_1, \dots, i_d) + T_2(i_1, \dots, i_d). \end{aligned} \quad (29)$$

Hence, the *addition* of tensors in the TR format can be performed by merging of their cores. \square

Note that the sizes of new cores are increased and not optimal in general. This problem can be solved by the rounding procedure [31].

Theorem 4.2. *Let $\mathcal{T} \in \mathbb{R}^{n_1 \times \dots \times n_d}$ be a d th-order tensor whose TR representation is $\mathcal{T} = \mathfrak{R}(\mathcal{Z}_1, \dots, \mathcal{Z}_d)$ and $\mathbf{u}_k \in \mathbb{R}^{n_k}, k = 1, \dots, d$ be a set of vectors, then the multilinear products, denoted by $c = \mathcal{T} \times_1 \mathbf{u}_1^T \times_2 \dots \times_d \mathbf{u}_d^T$, can be computed by multilinear product on each cores, which is*

$$c = \mathfrak{R}(\mathbf{X}_1, \dots, \mathbf{X}_d) \text{ where } \mathbf{X}_k = \sum_{i_k=1}^{n_k} \mathbf{Z}_k(i_k) u_k(i_k). \quad (30)$$

Proof. The *multilinear product* between a tensor and vectors can be expressed by

$$\begin{aligned} c &= \mathcal{T} \times_1 \mathbf{u}_1^T \times_2 \dots \times_d \mathbf{u}_d^T \\ &= \sum_{i_1, \dots, i_d} T(i_1, \dots, i_d) u_1(i_1) \dots u_d(i_d) \\ &= \sum_{i_1, \dots, i_d} \text{Tr} \left(\prod_{k=1}^d \mathbf{Z}_k(i_k) \right) u_1(i_1) \dots u_d(i_d) \\ &= \text{Tr} \left(\prod_{k=1}^d \left(\sum_{i_k=1}^{n_k} \mathbf{Z}_k(i_k) u_k(i_k) \right) \right). \end{aligned} \quad (31)$$

Thus, it can be written as a TR decomposition shown in (30) where each core $\mathbf{X}_k \in \mathbb{R}^{r_k \times r_{k+1}}$ becomes a matrix. The computational complexity is equal to $\mathcal{O}(dnr^2)$. \square

From (31), we can see that the multilinear product between \mathcal{T} and $\mathbf{u}_k, k = 1, \dots, d$ can be also expressed as an inner product of \mathcal{T} and the rank-1 tensor, i.e.,

$$\mathcal{T} \times_1 \mathbf{u}_1^T \times_2 \dots \times_d \mathbf{u}_d^T = \langle \mathcal{T}, \mathbf{u}_1 \circ \dots \circ \mathbf{u}_d \rangle. \quad (32)$$

It should be noted that the computational complexity in the original tensor form is $\mathcal{O}(dn^d)$, while it reduces to $\mathcal{O}(dnr^2 + dr^3)$ that is linear to tensor order d by using TR representation.

Theorem 4.3. *Let \mathcal{T}_1 and \mathcal{T}_2 be d th-order tensors of size $n_1 \times \dots \times n_d$. If the TR decompositions of these two tensors are $\mathcal{T}_1 = \mathfrak{R}(\mathcal{Z}_1, \dots, \mathcal{Z}_d)$ where $\mathcal{Z}_k \in \mathbb{R}^{r_k \times n_k \times r_{k+1}}$ and $\mathcal{T}_2 = \mathfrak{R}(\mathcal{Y}_1, \dots, \mathcal{Y}_d)$, where $\mathcal{Y}_k \in \mathbb{R}^{s_k \times n_k \times s_{k+1}}$, then the Hadamard product of these two tensors, $\mathcal{T}_3 = \mathcal{T}_1 \circledast \mathcal{T}_2$, can be also represented in the TR format given by $\mathcal{T}_3 = \mathfrak{R}(\mathcal{X}_1, \dots, \mathcal{X}_d)$, where $\mathcal{X}_k \in \mathbb{R}^{q_k \times n_k \times q_{k+1}}$ and $q_k = r_k * s_k$. Each core \mathcal{X}_k can be computed by*

$$\mathbf{X}_k(i_k) = \mathbf{Z}_k(i_k) \otimes \mathbf{Y}_k(i_k), \quad k = 1, \dots, d. \quad (33)$$

Proof. Each element in tensor \mathcal{T}_3 can be written as

$$\begin{aligned} T_3(i_1, \dots, i_d) &= T_1(i_1, \dots, i_d) T_2(i_1, \dots, i_d) \\ &= \text{Tr} \left(\prod_{k=1}^d \mathbf{Z}_k(i_k) \right) \text{Tr} \left(\prod_{k=1}^d \mathbf{Y}_k(i_k) \right) \\ &= \text{Tr} \left\{ \left(\prod_{k=1}^d \mathbf{Z}_k(i_k) \right) \otimes \left(\prod_{k=1}^d \mathbf{Y}_k(i_k) \right) \right\} \\ &= \text{Tr} \left\{ \prod_{k=1}^d \left(\mathbf{Z}_k(i_k) \otimes \mathbf{Y}_k(i_k) \right) \right\}. \end{aligned} \quad (34)$$

Hence, \mathcal{T}_3 can be also represented as TR format with its cores computed by (33), which costs $\mathcal{O}(dnq^2)$. \square

Furthermore, one can compute the *inner product* of two tensors in TR representations. For two tensors \mathcal{T}_1 and \mathcal{T}_2 , it is defined as

$$\langle \mathcal{T}_1, \mathcal{T}_2 \rangle = \sum_{i_1, \dots, i_d} T_3(i_1, \dots, i_d), \quad (35)$$

where $\mathcal{T}_3 = \mathcal{T}_1 \circledast \mathcal{T}_2$. Thus, the inner product can be computed by applying Hadamard product and then computing the multilinear product between \mathcal{T}_3 and vectors of all ones, i.e., $\mathbf{u}_k = \mathbf{1}, k = 1, \dots, d$. In contrast to $\mathcal{O}(n^d)$ in the original tensor form, the computational complexity

is equal to $\mathcal{O}(dnq^2 + dq^3)$ that is linear to d by using TR representation. Similarly, we can also compute *Frobenius norm* $\|\mathcal{T}\|_F = \sqrt{\langle \mathcal{T}, \mathcal{T} \rangle}$ in the TR representation.

In summary, by using TR representations, many important multilinear operations can be performed by operations on their cores with smaller sizes, resulting in that the computational complexity scales linearly to the tensor order.

5 RELATION TO OTHER MODELS

In this section, we discuss the relations between TR model and the classical tensor decompositions including CPD, Tucker and TT models. All these tensor decompositions can be viewed as the transformed representation of a given tensor. The number of parameters in CPD is $\mathcal{O}(dnr)$ that is linear to tensor order, however, its optimization problem is difficult and convergence is slow. The Tucker model is stable and can approximate an arbitrary tensor as close as possible, however, its number of parameters is $\mathcal{O}(dnr + r^d)$ that is exponential to tensor order. In contrast, TT and TR decompositions have similar representation power to Tucker model, while their number of parameters is $\mathcal{O}(dnr^2)$ that is linear to tensor order.

It should be noted that (i) TR model has a more generalized and powerful representation ability than TT model, due to relaxation of the strict condition $r_1 = r_{d+1} = 1$ in TT. In fact, TT decomposition can be viewed as a special case of TR model, as demonstrated in Sec. 5.3. (ii) TR-ranks are usually smaller than TT-ranks because TR model can be represented as a linear combination of TT decompositions whose cores are partially shared. (iii) TR model is more flexible than TT, because TR-ranks can be equally distributed in the cores, but TT-ranks have a relatively fixed pattern, i.e., smaller in border cores and larger in middle cores. (iv) Another important advantage of TR model over TT model is the circular dimensional permutation invariance (see Theorem 2.1). In contrast, the sequential multilinear products of cores in TT must follow a strict order such that the optimized TT cores highly depend on permutation of the original tensor.

5.1 CP decomposition

The canonical polyadic decomposition (CPD) aims to represent a d th-order tensor \mathcal{T} by a sum of rank-one tensors, given by

$$\mathcal{T} = \sum_{\alpha=1}^r \mathbf{u}_\alpha^{(1)} \circ \dots \circ \mathbf{u}_\alpha^{(d)}, \quad (36)$$

where each rank-one tensor is represented by an outer product of d vectors. It can be also written in the element-wise form given by

$$T(i_1, \dots, i_d) = \left\langle \mathbf{u}_{i_1}^{(1)}, \dots, \mathbf{u}_{i_d}^{(d)} \right\rangle, \quad (37)$$

where $\langle \cdot, \dots, \cdot \rangle$ denotes an inner product of a set of vectors, i.e., $\mathbf{u}_{i_k}^{(k)} \in \mathbb{R}^r, k = 1, \dots, d$.

By defining $\mathbf{V}_k(i_k) = \text{diag}(\mathbf{u}_{i_k}^{(k)})$ which is a diagonal matrix for each fixed i_k and k , where $k = 1, \dots, d, i_k = 1, \dots, n_k$, we can rewrite (37) as

$$T(i_1, \dots, i_d) = \text{Tr}(\mathbf{V}_1(i_1)\mathbf{V}_2(i_2) \cdots \mathbf{V}_d(i_d)). \quad (38)$$

Hence, CPD can be viewed as a special case of TR decomposition $\mathcal{T} = \mathfrak{R}(\mathcal{V}_1, \dots, \mathcal{V}_d)$ where the cores $\mathcal{V}_k, k = 1, \dots, d$ are of size $r \times n_k \times r$ and each lateral slice matrix $\mathbf{V}_k(i_k)$ is a diagonal matrix of size $r \times r$.

5.2 Tucker decomposition

The Tucker decomposition aims to represent a d th-order tensor \mathcal{T} by a multilinear product between a core tensor $\mathcal{G} \in \mathbb{R}^{r_1 \times \dots \times r_d}$ and factor matrices $\mathbf{U}^{(k)} \in \mathbb{R}^{n_k \times r_k}, k = 1, \dots, d$, which is expressed by

$$\mathcal{T} = \mathcal{G} \times_1 \mathbf{U}^{(1)} \times_2 \cdots \times_d \mathbf{U}^{(d)} = \llbracket \mathcal{G}, \mathbf{U}^{(1)}, \dots, \mathbf{U}^{(d)} \rrbracket. \quad (39)$$

By assuming the core tensor \mathcal{G} can be represented by a TR decomposition $\mathcal{G} = \mathfrak{R}(\mathcal{V}_1, \dots, \mathcal{V}_d)$, the Tucker decomposition (39) in the element-wise form can be rewritten as

$$\begin{aligned} T(i_1, \dots, i_d) &= \mathfrak{R}(\mathcal{V}_1, \dots, \mathcal{V}_d) \times_1 \mathbf{u}^{(1)T}(i_1) \times_2 \cdots \times_d \mathbf{u}^{(d)T}(i_d) \\ &= \text{Tr} \left\{ \prod_{k=1}^d \left(\sum_{\alpha_k=1}^{r_k} \mathbf{V}_k(\alpha_k) \mathbf{u}^{(k)}(i_k, \alpha_k) \right) \right\} \\ &= \text{Tr} \left\{ \prod_{k=1}^d \left(\mathcal{V}_k \times_2 \mathbf{u}^{(k)T}(i_k) \right) \right\}, \end{aligned} \quad (40)$$

where the second step is derived by applying Theorem 4.2. Hence, Tucker model can be represented as a TR decomposition $\mathcal{T} = \mathfrak{R}(\mathcal{Z}_1, \dots, \mathcal{Z}_d)$ where the cores are computed by the multilinear products between TR cores representing \mathcal{G} and the factor matrices, respectively, which is

$$\mathcal{Z}_k = \mathcal{V}_k \times_2 \mathbf{U}^{(k)}, \quad k = 1, \dots, d. \quad (41)$$

5.3 TT decomposition

The tensor train decomposition aims to represent a d th-order tensor \mathcal{T} by a sequence of cores $\mathcal{G}_k, k = 1, \dots, d$, where the first core $\mathbf{G}_1 \in \mathbb{R}^{n_1 \times r_2}$ and the last core $\mathbf{G}_d \in \mathbb{R}^{r_{d-1} \times n_d}$ are matrices while the other cores $\mathcal{G}_k \in \mathbb{R}^{r_k \times n_k \times r_{k+1}}, k = 2, \dots, d-1$ are 3rd-order tensors. Specifically, TT decomposition in the element-wise form is expressed as

$$T(i_1, \dots, i_d) = \mathbf{g}_1(i_1)^T \mathbf{G}_2(i_2) \cdots \mathbf{G}_{d-1}(i_{d-1}) \mathbf{g}_d(i_d), \quad (42)$$

where $\mathbf{g}_1(i_1)$ is the i_1 th row vector of \mathbf{G}_1 , $\mathbf{g}_d(i_d)$ is the i_d th column vector of \mathbf{G}_d , and $\mathbf{G}_k(i_k), k = 2, \dots, d-1$ are the i_k th lateral slice matrices of \mathcal{G}_k .

According to the definition of TR decomposition in (1), it is obvious that TT decomposition is a special case of TR decomposition where the first and the last cores are matrices, i.e., $r_1 = r_{d+1} = 1$. On the other hand, TR decomposition can be also rewritten as

$$\begin{aligned} T(i_1, \dots, i_d) &= \text{Tr} \{ \mathbf{Z}_1(i_1) \mathbf{Z}_2(i_2) \cdots \mathbf{Z}_d(i_d) \} \\ &= \sum_{\alpha_1=1}^{r_1} \mathbf{z}_1(\alpha_1, i_1, :)^T \mathbf{Z}_2(i_2) \cdots \mathbf{Z}_{d-1}(i_{d-1}) \mathbf{z}_d(:, i_d, \alpha_1) \end{aligned} \quad (43)$$

where $\mathbf{z}_1(\alpha_1, i_1, :) \in \mathbb{R}^{r_2}$ is the α_1 th row vector of the matrix $\mathbf{Z}_1(i_1)$ and $\mathbf{z}_d(:, i_d, \alpha_1)$ is the α_1 th column vector of the matrix $\mathbf{Z}_d(i_d)$. Therefore, TR decomposition can be interpreted as a sum of TT representations. The number of

TABLE 1

The functional data $f_1(x)$, $f_2(x)$, $f_3(x)$ is tensorized to 10th-order tensor ($4 \times 4 \times \dots \times 4$). In the table, ϵ , \bar{r} , N_p denote relative error, average rank, and the total number of parameters, respectively.

	$f_1(x)$				$f_2(x)$				$f_3(x)$				$f_1(x) + \mathcal{N}(0, \sigma), SNR = 60dB$			
	ϵ	\bar{r}	N_p	Time (s)	ϵ	\bar{r}	N_p	Time (s)	ϵ	\bar{r}	N_p	Time (s)	ϵ	\bar{r}	N_p	Time (s)
TT-SVD	3e-4	4.4	1032	0.17	3e-4	5	1360	0.16	3e-4	3.7	680	0.16	1e-3	16.6	13064	0.5
TR-SVD	3e-4	4.4	1032	0.17	3e-4	5	1360	0.28	5e-4	3.6	668	0.15	1e-3	9.7	4644	0.4
TR-ALS	3e-4	4.4	1032	13.2	3e-4	5	1360	18.6	8e-4	3.6	668	4.0	1e-3	4.4	1032	11.8
TR-ALSRA	7e-4	5	1312	85.15	2e-3	4.9	1448	150.5	4e-3	4.6	1296	170.0	1e-3	4.5	1100	64.8
TR-BALS	9e-4	4.3	1052	4.6	8e-4	4.9	1324	5.7	5e-4	3.7	728	3.4	1e-3	4.2	1000	6.1

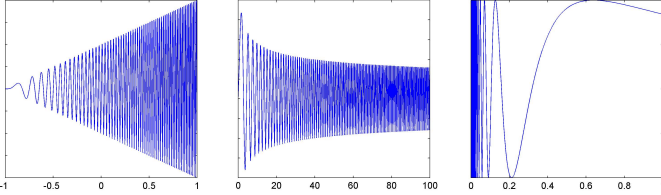


Fig. 2. Highly oscillated functions. The left panel is $f_1(x) = (x + 1)\sin(100(x + 1)^2)$. The middle panel is Airy function: $f_2(x) = x^{-\frac{1}{4}}\sin(\frac{2}{3}x^{\frac{3}{2}})$. The right panel is Chirp function $f_3(x) = \sin\frac{x}{4}\cos(x^2)$.

TT representations is r_1 and these TT representations have the common cores \mathcal{Z}_k , for $k = 2, \dots, d - 1$. In general, TR outperforms TT in terms of representation power due to the fact of linear combinations of a group of TT representations. Furthermore, given a specific approximation level, TR representation requires smaller ranks than TT representation.

6 EXPERIMENTAL RESULTS

In the following section we investigate the performance of the proposed TR model and algorithms, while also comparing it with the existing tensor decomposition models. We firstly conducted several numerical experiments on synthetic data to evaluate the effectiveness of our algorithms. Subsequently, two real-world datasets were employed to investigate the representation power of TR model together with classification performances. All computations were performed by a windows workstation with 3.33GHz Intel(R) Xeon(R) CPU, 64G memory and MATLAB R2012b.

6.1 Numerical experiments

In the first example, we consider highly oscillating functions that can be approximated well by a low-rank TT format [54], [55], as shown in Fig. 2. We firstly apply the reshaping operation to the functional vector resulting in a d th-order tensor of size $n_1 \times n_2 \times \dots \times n_d$, where isometric size is usually preferred, i.e., $n_1 = n_2 = \dots = n_d = n$, with the total number of elements denoted by $N = n^d$. This operation is also termed as *tensorization* or *n-folding representation* of the functional vector. We tested the TR model on these functional data by using four proposed algorithms (i.e., TR-SVD, TR-ALS, TR-ALSAR, TR-BALS) and compared with TT-SVD algorithm in terms of relative error ϵ , average rank \bar{r} , total number of parameters N_p and running time. In addition to three functional data, we also performed simulations on $f_1(x)$ when Gaussian noise was considered. We specify the error bound (tolerance), denoted

by $\epsilon_p = 10^{-3}$, as the stopping criterion for all compared algorithms. These algorithms can determine either TT-ranks or TR-ranks according to relative error tolerance ϵ_p except TR-ALS that requires manually given TR-ranks. We use TR-ranks obtained from TR-SVD algorithm as the setting of TR-ALS algorithm. Thus, we can compare the difference between TR approximations with orthogonal cores and non-orthogonal cores. As shown in Table 1, TR-SVD and TT-SVD obtain comparable results including relative error, average rank and number of parameters for approximation of $f_1(x)$, $f_2(x)$, $f_3(x)$, while TR-SVD outperforms TT-SVD on $f_1(x)$ with Gaussian noise, which requires much smaller average TR-ranks. This result indicates that TR-SVD can represent such data by smaller number of parameters N_p and effectively prevent overfitting the noise. The running time of TR-SVD and TT-SVD are comparable in all simulations. Although TR-ALS does not impose orthogonality constraints on cores, it can also achieve the same relative error with TR-SVD for approximation of $f_1(x)$, $f_2(x)$, $f_3(x)$, while its running time is longer than TR-SVD due to the iterative procedure. When Gaussian noise was considered, TR-ALS using fixed TR-ranks can effectively avoid overfitting to noise. Both TR-ALSAR and TR-BALS can adjust TR-ranks automatically based on error bound ϵ_p , however, TR-BALS outperforms TR-ALSAR in terms of relative error, average rank and running time. TR-BALS can obtain comparable results with TR-SVD for approximation of $f_1(x)$, $f_2(x)$, $f_3(x)$ and significantly outperforms TR-SVD when noise is involved. More detailed comparisons of these algorithms can be found in Table 1.

It should be noted that TT representation has the property that $r_1 = r_{d+1} = 1$ and $r_k, k = 2, \dots, d - 1$ are bounded by the rank of k -unfolding matrix of $\mathbf{T}_{(k)}$, which limits its generalization ability and consistence when the dimensions of tensor have been shifted or permuted. To demonstrate this, we consider to shift the dimensions of \mathcal{T} of size $n_1 \times \dots \times n_d$ by k times leading to $\overline{\mathcal{T}}^k$ of size $n_{k+1} \times \dots \times n_d \times n_1 \times \dots \times n_k$. We applied TT and TR decompositions to the dimension shifted data generated by $f_2(x)$, and compared different algorithms under all situations when $k = 1, \dots, 9$. As shown in Table 2, the average TT-ranks are varied dramatically along with the different shifts. In particular, when $k = 8$, \bar{r}_{tt} becomes 14.6, resulting in the large number of parameters $N_p = 10376$, which implies a very low compression ability. In contrast to TT decomposition, TR-SVD achieves slightly better performance in some cases but not for all cases. For TR-ALS, since TR-ranks were specified as $(r_{k+1}, \dots, r_d, r_1, \dots, r_k)$ for any k shifted cases, it achieves the consistent results.

TABLE 2

The results under different shifts of dimensions on functional data $f_2(x)$ with error bound setting to 10^{-3} . For the 10th-order tensor, all 9 dimension shifts were considered and the average rank \bar{r} as well as the number of total parameters N_p are compared.

	\bar{r}									N_p								
	1	2	3	4	5	6	7	8	9	1	2	3	4	5	6	7	8	9
TT-SVD	5.2	5.8	6	6.2	7	7	8.5	14.6	8.4	1512	1944	2084	2144	2732	2328	3088	10376	3312
TR-SVD	5.2	5.8	5.9	6.2	9.6	10	14	12.7	6.5	1512	1944	2064	2144	4804	4224	9424	7728	2080
TR-ALS	5	5	5	5	5	5	5	5	5	1360	1360	1360	1360	1360	1360	1360	1360	1360
TR-ALSAR	5.5	6.6	6.2	5.2	5.3	5.8	6.9	5.3	4.7	1828	2064	1788	1544	1556	1864	2832	1600	1324
TR-BALS	5	4.9	5	4.9	4.9	5	5	4.8	4.9	1384	1324	1384	1348	1348	1384	1384	1272	1324

However, the TR-ranks are usually unknown in practice, we must resort to TR-ALSAR and TR-BALS that can adapt TR-ranks automatically based on the error tolerance. As compared with TR-ALSAR, TR-BALS can obtain more compact representation together with smaller relative errors. In addition, TR-BALS can even outperform TR-ALS in several cases, implying that TR-ranks obtained from TR-SVD are not always the optimal one. More detailed results can be found in Table 2. These experiments demonstrate that TR decomposition is stable, flexible and effective for general data, while TT decomposition has strict limitations on data organization. Therefore, we can conclude that TR model is a more generalized and powerful representation with higher compression ability as compared to TT.

In the next experiment, we consider higher order tensors which are known to be represented well by TR model. We simplify the TR-ranks as $r_1 = r_2 = \dots = r_d$ that are varied from 1 to 4, $n_1 = n_2 = \dots = n_d = 4$ and $d = 10$. The cores, \mathcal{G}_k , ($k = 1, \dots, d$), were drawn from the normal distribution, which are thus used to generate a 10th-order tensor. We firstly apply different algorithms with the setting of $\epsilon_p = 10^{-3}$ to \mathcal{T} generated by using different ranks. Subsequently, we also consider Gaussian noise corrupted tensor $\mathcal{T} + \mathcal{N}(0, \sigma^2)$ with SNR=40dB and apply these algorithms with the setting of $\epsilon_p = 10^{-2}$. As shown in Table 3, the maximum rank of TT-SVD increases dramatically when the true rank becomes larger and is approximately r_{true}^2 , which thus results in a large number of parameters N_p (i.e., low compression ability). TR-SVD performs similarly to TT-SVD, which also shows low compression ability when the true rank is high. For TR-ALS, since the true rank is given manually, it shows the best result and can be used as the baseline to evaluate the other TR algorithms. In contrast to TT-SVD and TR-SVD, both TR-ALSAR and TR-BALS are able to adapt TR-ranks according to ϵ_p , resulting in the significantly lower rank reflected by r_{max} and lower model complexity reflected by N_p . As compared to TR-BALS, TR-ALSAR is prone to overestimate the rank and computation cost is relatively high. The experimental results show that TR-BALS can learn the TR-ranks correctly in all cases, and the number of parameters N_p are exactly equivalent to the baseline, meanwhile, the running time is also reasonable. For the noisy tensor data, we observe that TT-SVD and TR-SVD are affected significantly with r_{max} becoming 361 and 323 when true rank is only 1, which thus results in a poor compression ability. This indicates that TT-SVD and TR-SVD are sensitive to noise and prone to overfitting problems. By contrast, TR-ALS, TR-ALSAR, and TR-BALS obtain impres-

sive results that are similar to that in noise free cases. TR-ALSAR slightly overestimates the TR-ranks. It should be noted that TR-BALS can estimate the true rank correctly and obtain the best compression ratio as TR-ALS given true rank. In addition, TR-BALS is more computationally efficient than TR-ALSAR. In summary, TT-SVD and TR-SVD have limitations for representing the tensor data with symmetric ranks, and this problem becomes more severe when noise is considered. The ALS algorithm can avoid this problem due to the flexibility on distribution of ranks. More detailed results can be found in Table 3.

6.2 COIL-100 dataset



Fig. 3. The reconstruction of Coil-100 dataset by using TRSVD. The top row shows the original images, while the reconstructed images are shown from the second to sixth rows corresponding to $\epsilon=0.1, 0.2, 0.3, 0.4, 0.5$, respectively.

In this section, the proposed TR algorithms are evaluated and compared with TT and CP decompositions on Columbia Object Image Libraries (COIL)-100 dataset [56] that contains 7200 color images of 100 objects (72 images per object) with different reflectance and complex geometric characteristics. Each image can be represented by a 3rd-order tensor of size $128 \times 128 \times 3$ and then is downsampled to $32 \times 32 \times 3$. Hence, the dataset can be finally organized as a 4th-order tensor of size $32 \times 32 \times 3 \times 7200$. In Fig. 3, we show the reconstructed images under different relative errors $\epsilon \in \{0.1, \dots, 0.5\}$ which correspond to different set of TR-ranks \mathbf{r}_{TR} . Obviously, if \mathbf{r}_{TR} are small, the images are smooth and blurred, while the images are more sharp when \mathbf{r}_{TR} are larger. This motivates us to apply TR model to extract the abstract information of objects by using low-dimensional cores, which can be considered as the feature

TABLE 3

The detailed results on synthetic data of size $(n_1 \times n_2 \times \dots \times n_d)$ where $n_1 = \dots = n_d = 4$, $d = 10$, $\mathbf{r}_{true} = \{1, \dots, 4\}$. In the table, ϵ denotes relative error, r_{max} is the maximum rank, and N_p denotes the number of total parameters (i.e., model complexity). 'N/A' denotes that rank is specified manually as the true rank.

\mathbf{r}_{true}	Methods	Without Noise				Gaussian Noise (SNR=40dB)			
		ϵ	r_{max}	N_p	Time (s)	ϵ	r_{max}	N_p	Time (s)
1	TT-SVD	8e-15	1	40	0.12	8e-3	361	5e5	0.9
	TR-SVD	7e-15	1	40	0.14	8e-3	323	6e5	1.2
	TR-ALS	3e-14	N/A	40	1.10	1e-2	N/A	40	1.0
	TR-ALSAR	3e-14	1	40	2.29	1e-2	1	40	2.2
	TR-BALS	6e-15	1	40	0.95	1e-2	1	40	1.0
2	TT-SVD	2e-14	4	544	0.24	8e-3	362	5e5	0.9
	TR-SVD	2e-14	8	1936	0.49	7e-3	324	6e5	1.2
	TR-ALS	2e-7	N/A	160	3.1	1e-2	N/A	160	2.5
	TR-ALSAR	2e-5	4	284	5.70	1e-2	4	320	6.1
	TR-BALS	2e-5	2	160	1.17	1e-2	2	160	1.2
3	TT-SVD	2e-14	9	2264	0.30	8e-3	364	5e5	1.0
	TR-SVD	2e-14	18	7776	0.55	7e-3	325	6e5	1.2
	TR-ALS	9e-6	N/A	360	5.39	1e-2	N/A	360	4.7
	TR-ALSAR	8e-4	4	580	10.66	1e-2	4	608	11.8
	TR-BALS	9e-4	3	360	2.24	1e-2	3	360	2.4
4	TT-SVD	2e-14	16	6688	0.45	7e-3	395	6e5	1.2
	TR-SVD	4e-4	32	22352	0.66	7e-3	335	7e5	1.2
	TR-ALS	1e-6	N/A	640	14.00	1e-2	N/A	640	11.4
	TR-ALSAR	8e-4	7	1084	30.99	1e-2	7	1252	35.9
	TR-BALS	2e-4	4	640	3.90	1e-2	4	640	3.9

extraction approach. More specifically, the 4th TR core \mathcal{G}_4 of size $(r_4 \times 7200 \times r_1)$, can be used as the latent TR features while the subchain $\mathcal{G}^{\neq 4}$ can be considered as the basis of latent subspace. It should be emphasized that the feature extraction by TR decomposition has some essentially different characteristics. The number of features is determined by $r_4 \times r_1$, while the flexibility of subspace basis is determined by r_2, r_3 . This implies that we can obtain very different features even the number of features is fixed, by varying r_2, r_3 of TR-ranks that are related to the subspace basis. Therefore, TR decomposition might provide a flexible and effective feature extraction framework. In this experiment, we simply use relative error bound as the criterion to control TR ranks, however, TR ranks are also possible to be controlled individually according to the specific physical meaning of each dimension. We apply the proposed TR algorithms with the setting of $\epsilon_p \in \{0.2, \dots, 0.5\}$, then the core \mathcal{G}_4 is used as extracted features with reduced dimensions. Subsequently, we apply the K-nearest neighbor (KNN) classifier with $K=1$ for classification. For detailed comparisons, we randomly select a certain ratio $\rho = 50\%$ or $\rho = 10\%$ samples as the training set and the rest as the test set. The classification performance is averaged over 10 times of randomly splitting. In Table 4, we show the relative error, maximum rank, average rank and classification accuracy under two different settings. We can see that r_{max} of TT-SVD is mostly smaller than that of CP-ALS when their ϵ is in the same level, while r_{max} of TR decompositions are much smaller than TT-SVD and CP-ALS. This indicates that TR model can outperform TT and CP models in terms of compression ratio. The best classification performance of CP-ALS is 97.56% ($\rho = 50\%$) and 83.38% ($\rho = 10\%$), which corresponds to $\epsilon = 0.3$.

TT-SVD achieves the classification performance of 99.05% ($\rho = 50\%$) and 89.11% ($\rho = 10\%$) when $\epsilon \approx 0.2$. TR-SVD can achieve 99.19% ($\rho = 50\%$) and 89.89% ($\rho = 10\%$) when $\epsilon \approx 0.3$. It should be noted that, TR model, as compared to TT, can preserve the discriminant information well even when the fitting error is larger. For TR-ALS, TR-ALSAR, and TR-BALS, r_{max} is comparable to that of TT-SVD under the corresponding ϵ , while the classification performances are slightly worse than TR-SVD. More detailed results are compared in Table 4. This experiment demonstrates that TR and TT decompositions are effective for feature extractions and outperform the CP decomposition. In addition, TR decompositions achieve the best classification performances together with the best compression ability as compared to TT and CP decompositions.

6.3 KTH video dataset



Fig. 4. Video dataset consists of six types of human actions performed by 25 subjects in four different scenarios. From the top to bottom, six video examples corresponding to each type of actions are shown.

TABLE 4

The comparisons of different algorithms on Coil-100 dataset. ϵ , r_{max} , \bar{r} denote relative error, the maximum rank and the average rank, respectively. For classification task, the ratio of training samples $\rho = 50\%$, 10% were considered.

	ϵ	r_{max}	\bar{r}	Acc. (%) ($\rho = 50\%$)	Acc. (%) ($\rho = 10\%$)
CP-ALS	0.20	70	70	97.46	80.03
	0.30	17	17	97.56	83.38
	0.39	5	5	90.40	77.70
	0.47	2	2	45.05	39.10
TT-SVD	0.19	67	47.3	99.05	89.11
	0.28	23	16.3	98.99	88.45
	0.37	8	6.3	96.29	86.02
	0.46	3	2.7	47.78	44.00
TR-SVD	0.19	23	12.0	99.14	89.29
	0.28	10	6.0	99.19	89.89
	0.36	5	3.5	98.51	88.10
	0.43	3	2.3	83.43	73.20
TR-ALS	0.20	23	12.0	95.10	70.38
	0.30	10	6.0	97.32	80.71
	0.40	5	3.5	95.77	79.92
	0.47	3	2.3	65.73	52.25
TR-ALSRA	0.20	51	16.2	79.49	60.18
	0.30	11	6	93.11	79.48
	0.39	4	3	83.67	66.50
	0.47	2	2	76.02	62.79
TR-BALS	0.19	31	11	96.00	72.75
	0.29	13	7	96.41	74.32
	0.40	4	2	94.68	84.22
	0.45	2	1.5	88.30	76.86

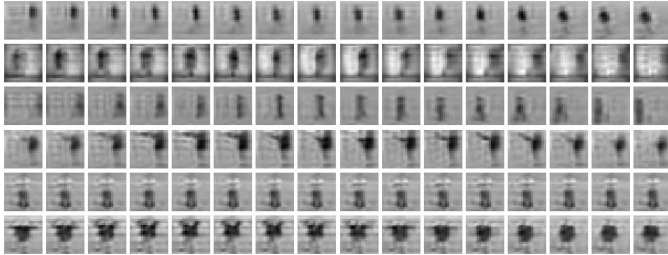


Fig. 5. The six examples of reconstructed video sequences by TR-BALS with $\epsilon = 0.27$, $r_{max} = 24$, $\bar{r} = 13.3$. The classification accuracy is 87.0% by using the cores obtained from TR-BALS.

In this section, we test the TR decompositions on KTH video database [57] containing six types of human actions (walking, jogging, running, boxing, hand waving and hand clapping) performed several times by 25 subjects in four different scenarios: outdoors, outdoors with scale variation, outdoors with different clothes and indoors as illustrated in Fig. 4. There are 600 video sequences for each combination of 25 subjects, 6 actions and 4 scenarios. Each video sequence was downsampled to $20 \times 20 \times 32$. Finally, we can organize the dataset as a tensor of size $20 \times 20 \times 32 \times 600$. We apply TR decompositions to represent the whole dataset by a set of 3rd-order TR cores, which can be also considered as the feature extraction or dimension reduction approach, and compare with TT and CP decompositions in terms of compression ability and classification performance. For extensive comparisons, we choose different error bound $\epsilon_p \in \{0.2, 0.3, 0.4\}$ for tensor decompositions. In Table 5, we can see that TR representations achieve better compression

TABLE 5

The comparisons of different algorithms on KTH dataset. ϵ denotes the obtained relative error; r_{max} denotes maximum rank; \bar{r} denotes the average rank; N_f denotes the total number of extracted features, and Acc. is the classification accuracy.

	ϵ	r_{max}	\bar{r}	N_f	Acc. (5×5 -fold)
CP-ALS	0.20	300	300	300	80.8 %
	0.30	40	40	40	79.3 %
	0.40	10	10	10	66.8 %
TT-SVD	0.20	139	78.0	139	84.8 %
	0.29	38	27.3	36	83.5 %
	0.38	14	9.3	9	67.8 %
TR-SVD	0.20	99	34.2	297	78.8 %
	0.29	27	12.0	81	87.7 %
	0.37	10	5.8	18	72.4 %
TR-ALS	0.30	27	12.0	81	87.3 %
	0.39	10	5.8	18	74.1 %
TR-ALSRA	0.29	29	16.0	39	82.3 %
	0.39	8	5.3	16	74.1 %
TR-BALS	0.27	24	13.3	100	87.0 %
	0.40	11	6	44	82.9 %

ratio reflected by smaller r_{max} , \bar{r} than that of TT-SVD, while TT-SVD achieves better compression ratio than CP-ALS. For instance, when $\epsilon \approx 0.2$, CP-ALS requires $r_{max} = 300$, $\bar{r} = 300$; TT-SVD requires $r_{max} = 139$, $\bar{r} = 78$, while TR-SVD only requires $r_{max} = 99$, $\bar{r} = 34.2$. For comparisons of different TR algorithms, we observe that TR-BALS outperforms the other algorithms in terms of compression ability. However, TR-ALSRA and TR-BALS cannot approximate data with any given error bound. For classification performance, we observe that the best accuracy (5×5 -fold cross validation) achieved by CP-ALS, TT-SVD, TR-SVD, TR-ALS, TR-ALSRA, TR-BALS are 80.8%, 84.8%, 87.7%, 87.3%, 82.3%, 87.0%, respectively. Note that these classification performances might not be the state-of-the-art on this dataset, however, we mainly focus on the comparisons among CP, TT, and TR decomposition frameworks. To obtain the best performance, we may apply the specific supervised feature extraction methods to TT or TR representations of dataset. It should be noted that TR decompositions achieve the best classification accuracy when $\epsilon = 0.3$, while TT-SVD and CP-ALS achieve their best classification accuracy when $\epsilon = 0.2$. This indicates that TR decomposition can preserve more discriminant information even when the approximation error is relatively high. Fig. 5 illustrates the reconstructed video sequences by TR-BALS, which corresponds to its best classification accuracy. Observe that although the videos are blurred and smooth, the discriminative information for action classification is still preserved. The detailed results can be found in Table 5. This experiment demonstrates that TR decompositions are effective for unsupervised feature representation due to their flexibility of TR-ranks and high compression ability.

7 CONCLUSION

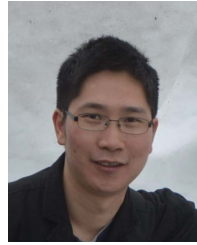
We have proposed a tensor decomposition model, which provides an efficient representation for a large-dimensional tensor by a sequence of low-dimensional cores. The number of parameters is $\mathcal{O}(dnr^2)$ that scales linearly to the tensor order. To optimize the latent cores, we have presented four dif-

ferent algorithms. In particular, TR-SVD is a non-recursive algorithm that is stable and efficient. TR-ALS is precise but requires TR-ranks to be given manually. TR-ALSAR and TR-BALS can adapt TR-ranks automatically with relatively high computational cost. Furthermore, we have investigated the properties on how the basic multilinear algebra can be performed efficiently by direct operations over TR representations (i.e., cores), which provides a potentially powerful framework for processing large-scale data. The relations to other tensor decomposition models are also investigated, which allows us to conveniently transform the latent representations from the traditional models to TR model. The experimental results have verified the effectiveness of the proposed TR model and algorithms.

REFERENCES

- [1] T. Kolda and B. Bader, "Tensor decompositions and applications," *SIAM Review*, vol. 51, no. 3, pp. 455–500, 2009.
- [2] A. Cichocki, D. Mandic, C. Caiafa, A.-H. Phan, G. Zhou, Q. Zhao, and L. D. Lathauwer, "Tensor decompositions for signal processing applications: From two-way to multiway component analysis," *IEEE Signal Processing Magazine*, vol. 32, no. 2, pp. 145–163, 2015.
- [3] R. Bro, "PARAFAC. Tutorial and applications," *Chemometrics and intelligent laboratory systems*, vol. 38, no. 2, pp. 149–171, 1997.
- [4] De Lathauwer, L., "A link between the canonical decomposition in multilinear algebra and simultaneous matrix diagonalization," *SIAM J. Matrix Anal. Appl.*, vol. 28, pp. 642–666, August 2006.
- [5] P. Comon, "Tensors, usefulness and unexpected properties," in *IEEE Workshop on Statistical Signal Processing, Cardiff, UK, (keynote)*. IEEE SP, 2009, pp. 781–788.
- [6] J. Goulart, M. Boizard, R. Boyer, G. Favier, and P. Comon, "Tensor cp decomposition with structured factor matrices: Algorithms and performance," *IEEE Journal of Selected Topics in Signal Processing*, 2015.
- [7] L. R. Tucker, "Some mathematical notes on three-mode factor analysis," *Psychometrika*, vol. 31, no. 3, pp. 279–311, 1966.
- [8] L. De Lathauwer, B. De Moor, and J. Vandewalle, "On the best rank-1 and rank-(R1,R2,...,RN) approximation of higher-order tensors," *SIAM J. Matrix Anal. Appl.*, vol. 21, pp. 1324–1342, 2000.
- [9] I. Oseledets, D. Savostyanov, and E. Tyrtshnikov, "Tucker dimensionality reduction of three-dimensional arrays in linear time," *SIAM J. Matrix Analysis Applications*, vol. 30, no. 3, pp. 939–956, 2008.
- [10] T. Yokota, R. Zdunek, A. Cichocki, and Y. Yamashita, "Smooth nonnegative matrix and tensor factorizations for robust multi-way data analysis," *Signal Processing*, vol. 113, pp. 234–249, 2015.
- [11] C. F. Caiafa and A. Cichocki, "Computing sparse representations of multidimensional signals using Kronecker bases," *Neural computation*, vol. 25, no. 1, pp. 186–220, 2013.
- [12] Z. He, A. Cichocki, S. Xie, and K. Choi, "Detecting the number of clusters in n -way probabilistic clustering," *IEEE Transactions on Pattern Analysis and Machine Intelligence*, vol. 32, no. 11, pp. 2006–2021, 2010.
- [13] T. Acar, Y. Yu, and A. P. Petropulu, "Blind mimo system estimation based on PARAFAC decomposition of higher order output tensors," *IEEE Trans. on Signal Processing*, vol. 54, no. 11, pp. 4156–4168, 2006.
- [14] C. Beckmann and S. Smith, "Tensorial extensions of independent component analysis for multisubject fmri analysis," *NeuroImage*, vol. 25, no. 1, pp. 294–311, 2005.
- [15] H.-S. Lee and D. Kim, "Tensor-based AAM with continuous variation estimation: Application to variation-robust face recognition," *IEEE Trans. Pattern Anal. Mach. Intell.*, vol. 31, no. 6, pp. 1102–1116, 2009.
- [16] Z. Xu, F. Yan, and A. Qi, "Infinite Tucker decomposition: Nonparametric Bayesian models for multiway data analysis," in *Proceedings of the 29th International Conference on Machine Learning (ICML-12)*, 2012, pp. 1023–1030.
- [17] G. Zhou, A. Cichocki, Q. Zhao, and S. Xie, "Efficient nonnegative Tucker decompositions: Algorithms and uniqueness," *Image Processing. IEEE Transactions on*, vol. 24, no. 12, pp. 4990–5003, 2015.
- [18] G. Zhou, Q. Zhao, Y. Zhang, T. Adali, S. Xie, and A. Cichocki, "Linked component analysis from matrices to high-order tensors: Applications to biomedical data," *Proceedings of the IEEE*, vol. 104, no. 2, pp. 310–331, 2016.
- [19] Y. Zhang, G. Zhou, Q. Zhao, J. Jin, X. Wang, and A. Cichocki, "ERP classification via spatial-temporal discriminant analysis: Reducing the calibration time for BCI," *IEEE Transactions on Neural Systems and Rehabilitation Engineering*, p. (submitted), 2012.
- [20] F. Miwakeichi, E. Martnez-Montes, P. Valds-Sosa, N. Nishiyama, H. Mizuhara, and Y. Yamaguchi, "Decomposing EEG data into space–time–frequency components using parallel factor analysis," *NeuroImage*, vol. 22, no. 3, pp. 1035–1045, 2004.
- [21] Q. Zhao, L. Zhang, and A. Cichocki, "Bayesian CP factorization of incomplete tensors with automatic rank determination," *IEEE Transactions on Pattern Analysis and Machine Intelligence*, vol. 37, no. 9, pp. 1751–1763, 2015.
- [22] Q. Zhao, G. Zhou, L. Zhang, A. Cichocki, and S. I. Amari, "Bayesian robust tensor factorization for incomplete multiway data," *IEEE Transactions on Neural Networks and Learning Systems*, vol. 27, no. 4, pp. 736–748, April 2016.
- [23] R. Orús, "A practical introduction to tensor networks: Matrix product states and projected entangled pair states," *Annals of Physics*, vol. 349, pp. 117–158, 2014.
- [24] T. Huckle, K. Waldherr, and T. Schulte-Herbriggens, "Computations in quantum tensor networks," *Linear Algebra and its Applications*, vol. 438, no. 2, pp. 750–781, 2013.
- [25] S. Sachdev, "Tensor networks—a new tool for old problems," *Physics*, vol. 2, p. 90, Oct 2009. [Online]. Available: <http://link.aps.org/doi/10.1103/Physics.2.90>
- [26] V. Murg, F. Verstraete, R. Schneider, P. Nagy, and O. Legeza, "Tree tensor network state with variable tensor order: An efficient multireference method for strongly correlated systems," *Journal of Chemical Theory and Computation*, vol. 11, no. 3, pp. 1027–1036, 2015.
- [27] A. Cichocki, "Era of big data processing: A new approach via tensor networks and tensor decompositions, (invited)," in *Proc. of Int. Workshop on Smart Info-Media Systems in Asia (SISA2013), Nagoya, Japan, Sept.30–Oct.2, 2013*. [Online]. Available: <http://arxiv.org/abs/1403.2048>
- [28] R. Hübener, V. Nebendahl, and W. Dür, "Concatenated tensor network states," *New Journal of Physics*, vol. 12, no. 2, p. 025004, 2010.
- [29] M. Espig, W. Hackbusch, S. Handschuh, and R. Schneider, "Optimization problems in contracted tensor networks," *Computing and Visualization in Science*, vol. 14, no. 6, pp. 271–285, 2011.
- [30] I. Oseledets and E. Tyrtshnikov, "TT-cross approximation for multidimensional arrays," *Linear Algebra and its Applications*, vol. 432, no. 1, pp. 70–88, 2010.
- [31] I. V. Oseledets, "Tensor-train decomposition," *SIAM Journal on Scientific Computing*, vol. 33, no. 5, pp. 2295–2317, 2011.
- [32] S. Holtz, T. Rohwedder, and R. Schneider, "The alternating linear scheme for tensor optimization in the tensor train format," *SIAM J. Scientific Computing*, vol. 34, no. 2, 2012.
- [33] L. Grasedyck, "Hierarchical singular value decomposition of tensors," *SIAM J. Matrix Analysis Applications*, vol. 31, no. 4, pp. 2029–2054, 2010.
- [34] J. Ballani, L. Grasedyck, and M. Kluge, "Black box approximation of tensors in hierarchical Tucker format," *Linear Algebra and its Applications*, vol. 438, no. 2, pp. 639–657, 2013.
- [35] A. Novikov and R. Rodomanov, "Putting MRFs on a tensor train," in *Proceedings of the International Conference on Machine Learning (ICML-14)*, 2014.
- [36] S. Dolgov, B. Khoromskij, and I. Oseledets, "Fast solution of parabolic problems in the tensor train/quantized tensor train format with initial application to the Fokker–Planck equation," *SIAM Journal on Scientific Computing*, vol. 34, no. 6, pp. A3016–A3038, 2012.
- [37] E. Jeckelmann, "Dynamical density-matrix renormalization-group method," *Physical Review B*, vol. 66, no. 4, p. 045114, 2002.
- [38] S. Dolgov, B. Khoromskij, I. Oseledets, and D. Savostyanov, "Computation of extreme eigenvalues in higher dimensions using block tensor train format," *Computer Physics Communications*, vol. 185, no. 4, pp. 1207–1216, 2014.
- [39] D. Kressner, M. Steinlechner, and A. Uschmajew, "Low-rank tensor methods with subspace correction for symmetric eigenvalue problems," *SIAM Journal on Scientific Computing*, vol. 36, no. 5, pp. A2346–A2368, 2014.

- [40] N. Lee and A. Cichocki, "Estimating a few extreme singular values and vectors for large-scale matrices in Tensor Train format," *SIAM Journal on Matrix Analysis and Applications*, vol. 36, no. 3, pp. 994–1014, 2015.
- [41] S. V. Dolgov and D. V. Savostyanov, "Alternating minimal energy methods for linear systems in higher dimensions," *SIAM Journal on Scientific Computing*, vol. 36, no. 5, pp. A2248–A2271, 2014.
- [42] B. N. Khoromskij, " $o(d \log n)$ -quantics approximation of N-d tensors in high-dimensional numerical modeling," *Constructive Approximation*, vol. 34, no. 2, pp. 257–280, 2011.
- [43] I. V. Oseledets, "Approximation of $2^d \times 2^d$ matrices using tensor decomposition," *SIAM Journal on Matrix Analysis and Applications*, vol. 31, no. 4, pp. 2130–2145, 2010.
- [44] S. Dolgov and B. Khoromskij, "Two-level QTT-tucker format for optimized tensor calculus," *SIAM Journal on Matrix Analysis and Applications*, vol. 34, no. 2, pp. 593–623, 2013.
- [45] O. Lebedeva, "Tensor conjugate-gradient-type method for rayleigh quotient minimization in block QTT-format," *Russian journal of numerical analysis and mathematical modelling*, vol. 26, no. 5, pp. 465–489, 2011.
- [46] S. Dolgov, B. Khoromskij, and D. Savostyanov, "Superfast fourier transform using QTT approximation," *Journal of Fourier Analysis and Applications*, vol. 18, no. 5, pp. 915–953, 2012.
- [47] T. Rohwedder and A. Uschmajew, "On local convergence of alternating schemes for optimization of convex problems in the tensor train format," *SIAM Journal on Numerical Analysis*, vol. 51, no. 2, pp. 1134–1162, 2013.
- [48] L. Grasedyck, M. Kluge, and S. Krämer, "Variants of alternating least squares tensor completion in the tensor train format," *SIAM Journal on Scientific Computing*, vol. 37, no. 5, pp. A2424–A2450, 2015.
- [49] M. Steinlechner, "Riemannian optimization for high-dimensional tensor completion," Technical report MATHICSE 5.2015, EPF Lausanne, Switzerland, Tech. Rep., 2015.
- [50] A. Novikov, D. Podoprikin, A. Osokin, and D. P. Vetrov, "Tensorizing neural networks," in *Advances in Neural Information Processing Systems*, 2015, pp. 442–450.
- [51] J. A. Bengua, H. N. Phien, H. D. Tuan, and M. N. Do, "Matrix product state for feature extraction of higher-order tensors," *arXiv preprint*, 2016.
- [52] H. N. Phien, H. D. Tuan, J. A. Bengua, and M. N. Do, "Efficient tensor completion: Low-rank tensor train," *arXiv preprint arXiv:1601.01083*, 2016.
- [53] D. Perez-Garcia, F. Verstraete, M. M. Wolf, and J. I. Cirac, "Matrix product state representations," *arXiv preprint quant-ph/0608197*, 2006.
- [54] B. N. Khoromskij, "Tensor numerical methods for multidimensional PDEs: theoretical analysis and initial applications," *ESAIM: Proceedings and Surveys*, vol. 48, pp. 1–28, 2015.
- [55] B. N. Khoromskij and S. I. Repin, "A fast iteration method for solving elliptic problems with quasiperiodic coefficients," *Russian Journal of Numerical Analysis and Mathematical Modelling*, vol. 30, no. 6, pp. 329–344, 2015.
- [56] S. Nayar, S. Nene, and H. Murase, "Columbia object image library (coil 100)," *Department of Comp. Science, Columbia University, Tech. Rep. CUCS-006-96*, 1996.
- [57] I. Laptev and T. Lindeberg, "Local descriptors for spatio-temporal recognition," in *Spatial Coherence for Visual Motion Analysis*. Springer, 2006, pp. 91–103.



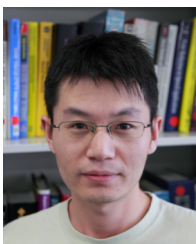
Guoxu Zhou received the Ph.D degree in intelligent signal and information processing from South China University of Technology, Guangzhou, China, in 2010. He is currently a research scientist of the laboratory for Advanced Brain Signal Processing, at RIKEN Brain Science Institute (JAPAN). His research interests include statistical signal processing, tensor analysis, intelligent information processing, and machine learning.



Liqing Zhang received the Ph.D. degree from Zhongshan University, Guangzhou, China, in 1988. He is now a Professor with Department of Computer Science and Engineering, Shanghai Jiao Tong University, Shanghai, China. His current research interests cover computational theory for cortical networks, visual perception and computational cognition, statistical learning and inference. He has published more than 210 papers in international journals and conferences.



Andrzej Cichocki received the Ph.D. and Dr.Sc. (Habilitation) degrees, all in electrical engineering, from Warsaw University of Technology (Poland). He is the senior team leader of the Laboratory for Advanced Brain Signal Processing, at RIKEN BSI (Japan). He is coauthor of more than 400 scientific papers and 4 monographs (two of them translated to Chinese). He served as AE of IEEE Trans. on Signal Processing, TNNLS, Cybernetics and J. of Neuroscience Methods.



Qibin Zhao received the Ph.D. degree from Department of Computer Science and Engineering, Shanghai Jiao Tong University, Shanghai, China, in 2009. He is currently a research scientist at Laboratory for Advanced Brain Signal Processing in RIKEN Brain Science Institute, Japan and is also a visiting professor in Saitama Institute of Technology, Japan. His research interests include machine learning, tensor factorization, computer vision and brain computer interface. He has published more than 50 papers in inter-

national journals and conferences.